

Geothermal Characteristics of Amguid Messaoud Oil Basin in Southern Algeria

Nabil Toumi¹, Aziez Zeddouri^{*1}

¹Laboratory of underground reservoirs of oil, gas, and aquifers, University of Kasdi Merbah Ouargla, road of Ghardaia, BP.511, 30 000, Algeria.

*e-mail: aziez.zeddouri@univ-ouargla.dz

Received : 20-01-2023 Accepted: 30-03-2023 Published : 01-04-2023

Abstract

In this work, we used the thermal resistance algorithm to calculate the true formation temperatures in Agued Messaoud Basin, located in the central-eastern part of the Algerian Sahara, using data provided by oil companies. Bottom temperatures were obtained for 234 wells from various in formation records. Calculations were performed on 10 wells possessing records with complete information, as well as records for the temperature correction due to drilling effects. Then heat flux (HF) maps and 3D models for each geological formation were established. These maps and models are intended to show the differences across the basin associated with thermal and geological changes. To obtain the formation thickness needed for thermal resistance calculations, all the formation contacts as polynomial surfaces of the 10 wells. We found an average basin HF ranging from 50 to 69 mW/m² and an average geothermal gradient of about 2.375°C/100m which is consistent with previous studies in the central and northern Algerian Sahara.

Keywords: Bottom-hole temperature; Geothermal gradient; heat flux; temperature correction, Thermal conductivity; Amguid Messaoud (key words).

Tob Regul Sci.™ 2023; 9(2): 2768 - 2782

DOI: doi.org/10.18001/TRS.9.2.182

Introduction

Heat flow studies are essential for understanding many fundamental geological and geophysical processes, such as plate tectonics and magmatic activity. heat flux (HF) also provides insight into hydrocarbon maturation and migration and groundwater flow.

Estimating subsurface temperatures requires knowledge of the surface temperature and thermal conductivity (TC) of a geologic section. The surface temperature can be estimated based on altitude and latitude.

TC can be measured directly by sampling from different geological strata or estimated based on the values of the common or dominant rocks in the stratigraphic column [1].

Generally, the necessary geothermal data are only available for wells specifically designed for heat flow measurements. Bottom hole temperatures (BHT) measured when drilling oil and gas wells reflects the thermal conditions in the borehole and is affected by mud turbulence. Inside the well, the drilling mud is colder than the drilled formations, so it tends to cool the rock near the bottom of the hole and heat the rock near the top [2]; [3]. The difference between the equilibrium temperature of the mud and rock depends on various factors such as the depth of the formation, the time required to drill, the natural thermal gradient, the porosity of the formation, the radius of the hole, the thermal conductivity of each rock, and the time between the end and the beginning of the drilling mud rotation record [4]. Unfortunately, the BHT is measured shortly after the drilling of the well is stopped and under unbalanced conditions. Moreover, there is no assessment of the accuracy of the tool or identification of data acquisition and recording problems. In addition, in many cases, there is no database where BHT values are readily available, nor is there information on the drilling and rotation system. When the necessary information is available, it can be applied to the BHT correction to calculate the true formation temperature [5]; [6]; [7]. Several methods and algorithms have been used to calculate the equilibrium temperature, some of which focus on the bottom-hole conditions when measuring the BHT value while others simulate the temperature change over the entire mud column (DST) [8]; [9].

Due to the multiple uses of geothermal energy, such as heating, fish farming, and mineral water treatment, along with industrial applications, this form of energy is one of Algeria's most important renewable sources. But although the potential of geothermal resources in northern Algeria is well defined, no detailed studies of southern Algeria have been conducted so far. The main objective of this study is to assess the geothermal potential in the Amguid Messaoud basin in southeast Algeria by calculating the subsurface temperatures in oil and gas wells based on oil company data, and map the present-day heat fluxes.

2. Geological Setting of The Study Area

The Hassi Messaoud region is famous for its vast oil-producing field and is situated within the Amguid Messaoud mole. This area is located in the southeastern part of Algeria, between latitudes 31° and 33° E and longitudes 5° and 7°30' N (Fig. 1). The entire region covers an area of 157793 km² [10].

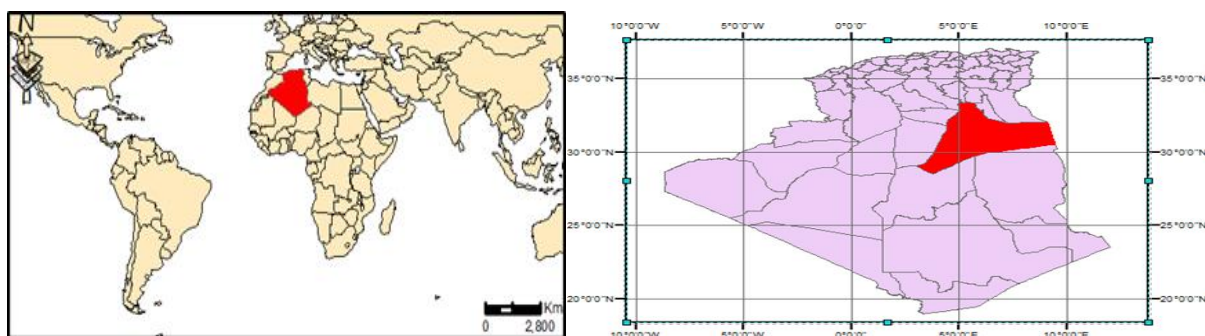


Fig. 1. Location of the Amguid Messaoud field in Ouargla Province (Algeria).

The AmguidMessaoud basin is located in the Saharan platform, which is part of the North African Craton and from a geological perspective situated south of the Algerian Alpine The bedrock of the Sahara region consists of ancient sedimentary and volcanic terrains that crop out in the Reguibat Shield to the west and the Targui Shield to the south [11].

Above the Precambrian basement, there is a strong unconformity beneath the sedimentary cover. During the Paleozoic era, this cover was deformed into multiple basins that were separated by elevated regions [12].

The stratigraphy of the study area (Fig. 2) includes two main sedimentary rock units(Paleozoic and Meso-Cenozoic) separated by the Hercynian unconformity; all resting on ametamorphic Precambrian basement [10]. dune chains cover theplatform, such is the case for the Great Western and Eastern Ergs, and Chech Erg.

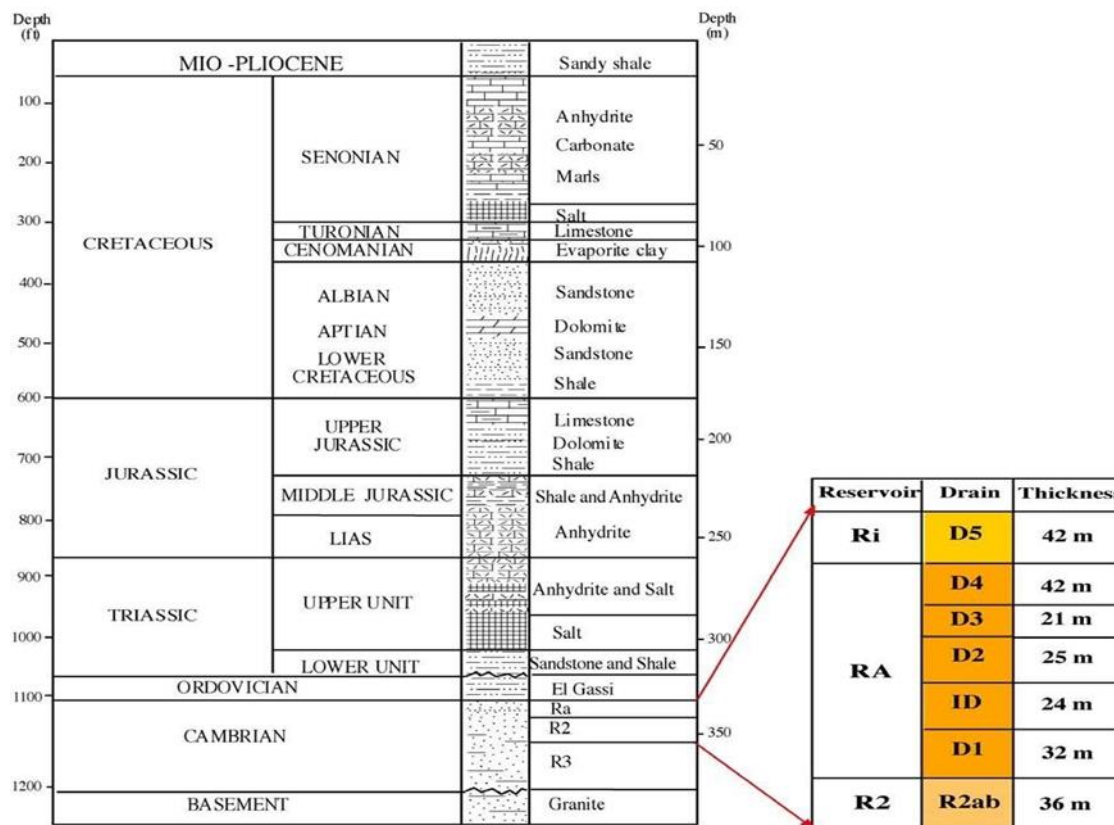


Fig. 2. Stratigraphy of the study area. Left side: Summarized stratigraphy for the HassiMessaoud field. Right side: Detailed column of the four productive zones R3, R2, Ra, Ri of the Cambrian of HassiMessaoud field [13]

3. Materials and Methods

3.1. Methodology and Acquisition of Temperature Data

The study of subsurface temperatures of a basin requires a systematic inventory of all data acquired from the reconnaissance work of oil drilling. The process for handling temperature data is outlined in the flow chart presented in Figure 3.

3.2. Used Data

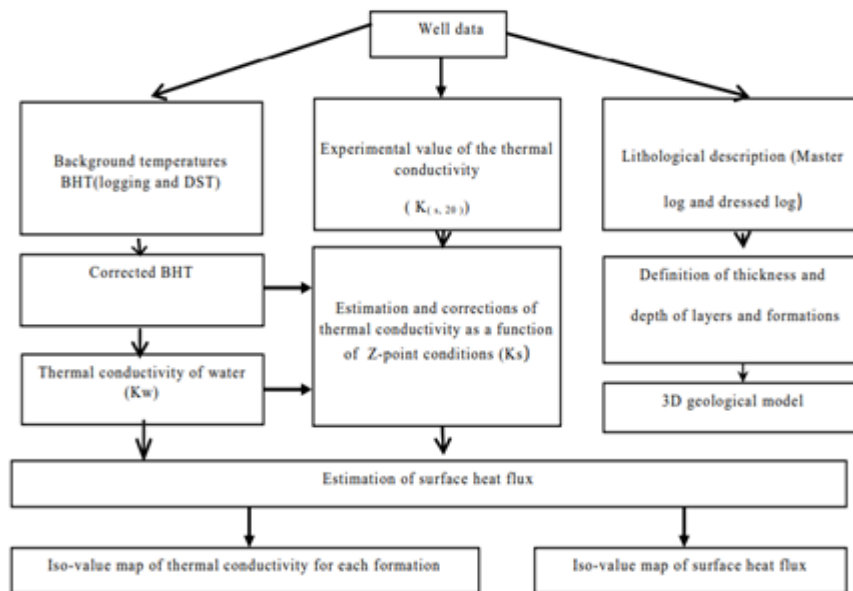


Fig. 3. Flowchart of the logical treatment of the problem.

Detailed temperature data are extracted from Sonatrach Oil and Gas company documents and reports drilling stem test temperature data (DST). BHT is turbulent and does not represent the true formation temperatures(logging and DST). The turbulent temperatures (BHT) must be corrected using one of the correction algorithms such as those used by [14]; [15]; [16].

In this work, the Horner technique used by Lachenbruch was adopted [14]. This is a commonly used method for correcting the BHT and for calculating the surface HF.

This technique gives the value of the TC as a function of the conditions at any point of depth Z and in particular as a function of TC experimental value $(K(s,20))$ and the nature and thickness of the rock formations described from the master-logs and logs of the boreholes. After the calculation and obtaining of the results and with the help of a software program (Rockworks16), it is possible to establish the iso-value maps of the TC for each formation and the iso-value map of the surface HF and the three-dimensional models of each layer.

4. Thermal Model for Heat Flux Calculation

4.1. BHT Correction

The heat flux calculation of the basin allows calculating the temperature at any depth. The HF was calculated by integrating the measurements of the well logs provided by Sonatrach and TC values determined in the laboratory at 20°C $(K(s,20))$ from the works of [17];[18]. To correct the TC of

each geological formation, this non-turbulent temperature correction requires at least (two measurements) of BHT and is more reliable if several measurements of BHT with time are integrated for corrections [19]; [20]. The correction method consists of plotting the BHT against time function according to the equation [19]; [9].

$$TB(t)=T(B,\infty)+A.\log((tc+te)/te). \quad (1)$$

Where:

tc is the circulation time; te is the time elapsed since the circulation; $TB(t)$: is the time-dependent (BHT) By plotting the $A.\log((tc+te)/te)$ versus T , we can estimate $T(B,\infty)$ the actual formation temperature were measured at depths of about 4000 m.

The following table (table 01) represents the results of the turbulent temperature correction (BHT) for each selected well using two measurements after plotting the linear slope and determining the value of each of A and $T(B, \infty)$ and measuring the bottom temperatures.

Table 1. temperature values and correction results.

Wells	Point 01	Point 02	BHT corrected in (°C)
	True BHT1 in (°C)	True BHT2 in (°C)	
BBR-2	113.460	115.000	115.400
BEK-1	122.000	124.000	124.700
BRS-3bis	121.808	121.846	122.600
HAB-1	122.292	122.254	123.100
HTBF-1	115.664	115.769	118.000
NBOG-1bis	102.000	101.000	102.400
RAA-1	118.000	119.000	119.100
RAMA-1	114.472	114.587	117.100
WRDC-2bis	114.000	121.000	124.300
ZMT-1	102.000	102.900	103.500

4 . 2. Calculation of The Heat Flux

We used TC values determined in the laboratory at 20°C (K(s,20)) and the TC of water(Kw) to correct the TC (Kr) for each point. For the geological formation as a function of depth, and taking into account the correct temperature and porosity of the formation, we relate TC with porosity according to the equation [21]; [22]:

$$K_r = K_w \cdot \phi \cdot K_s (1 - \phi) \quad (2)$$

Ks: the conductivity of the solid matrix.

Assuming that the pores are filled with water, the conductivity of water is 0.56 W/m.kat 0°C, but it increases to 0.68 W/m.kat 100°C. We used the approximate water temperature and conductivity data provided by [23]; [65]; [24] with the following functions:

$$K_w = 0.56 + 0.003 \cdot T \cdot 0.827. \text{ For } 0 \leq T \leq 63^\circ\text{C}. \quad (3)$$

$$K_w = 0.481 + 0.942 \cdot \ln(T). \text{ For } T > 63^\circ\text{C}. \quad (4)$$

These equations were then used to adjust (Kw) for in situ conditions in the basin. We further assumed that the conductivity (Ks) of the solid matrix is proportional to the reciprocal of the absolute temperature, such that:

$$K_s = K(s, 20) [293 / (279 + T)]. \quad (5)$$

Where

The following relationship was used to calculate the HF values for each site:

$$q_0(x, y) = [T_0(B, \infty)(x, y) - T_0] / \sum_{Z=0}^B [(\Delta Z(x, y)) / (k(x, y, z, \phi, T))] \quad (6)$$

For each well, the latitude and longitude (equivalent to x and y), the corrected downhole temperature T(B,∞) and the corresponding depth Z=B were stored in a data file. The surface temperature as a function of position T0(x,y), rock thickness Δz(x, y) as a function of position, and TC, K(x, y, z, φ, T) as a function of position and depth were calculated from empirical functions [21]; [1]; [25].

5. Results and Discussions

5.1. 3 D Blocks of the Bottom Hole Temperature (BHT)

To get an idea of the evolution of temperature with depth in the AmguidMessaoud basin, 3D models and maps were drawn as shown in Figure 04:

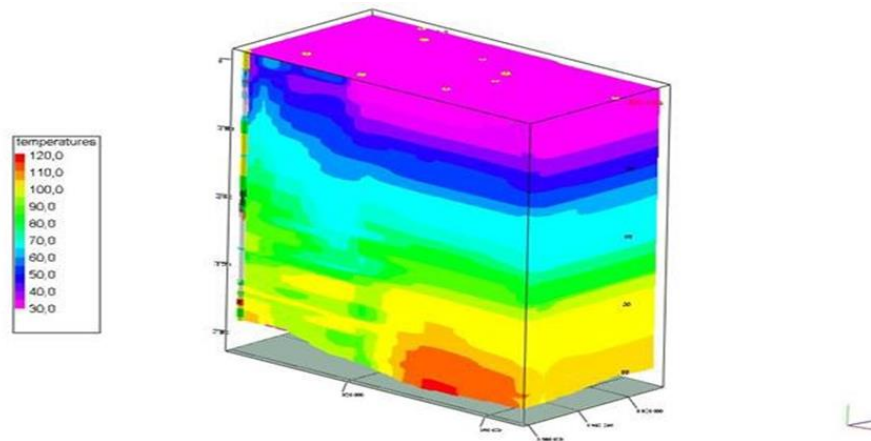


Fig. 4. 3D block of the BHT bottom temperature.

The temperature of the rocks increases with depth; this is called the geothermal gradient, which varies with the layers of rocks that the wells intersect. Because oil and gas wells are deep and cover a large portion of the basin, they provide better geothermal gradient data. Geothermal gradient mapping and 3D modeling have permitted us to better understand geothermal changes in the basin. The temperature at each point in the study area can be predicted as a function of depth [26]; [27]; [22] using the following (geothermal gradient) formula:

$$G = DT/D(^{\circ}C/100m). \quad (7)$$

Where

T: Temperature ($^{\circ}C$). Z: Depth (m).

5.2. Interpretation of The Geothermal Gradient Map

After correcting the BHT values and redrawing the temperature profile for each oil well, the average geothermal gradient obtained is $2.375^{\circ}C/100m$. This value is low compared to previous studies which found an average of $3^{\circ}C/100m$ but without BHT correction. We start reading the evolution of the values of the Geothermal Gradient Map (Fig. 5) after correction (BHT) from east to west, where we find the lowest value of geothermal gradient $2.1^{\circ}C/100m$ at RAMA-1 in Rhourd el Amar-1 and also as we move eastward until we reach the NBOG-1bis well and all the surrounding area called North Bougoufa and it further increases until reaching $2.33^{\circ}C/100m$ in the North-West of the basin in the BBR-2 well (BouRouicha area) with a maximum of $2.65^{\circ}C/100m$ as the recorded value of the temperature gradient in the WRDC-2BIS well in the RhourdeChegga area at the extreme south-west of the AmguidMessaoud basin.

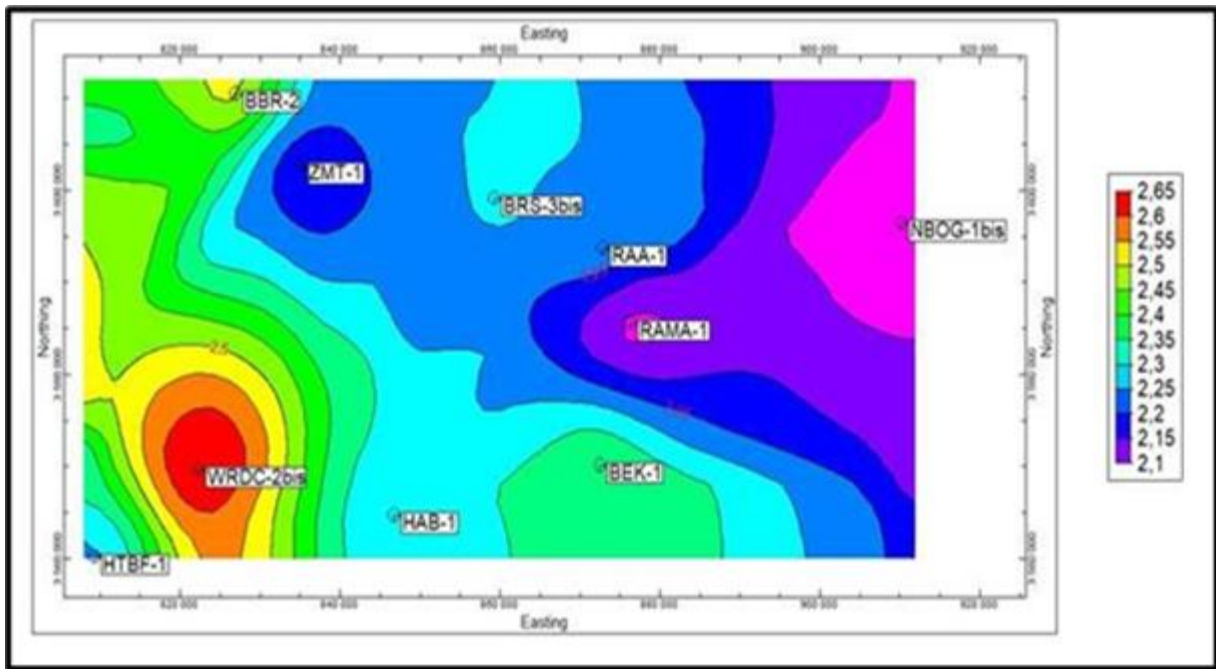


Fig. 5. The geothermal gradient map of the northern AmguidMessaoud mole.

5.3. 3D Block of Thermal Conductivity

Using the TC at each point of the wells in the basin formation and using Rockworks 16 software we drew 3D models, TC maps as well as the heat flow of the basin to obtain a correct and accurate interpretation of each formation. According to the three-dimensional model of the TC of the basin (Fig. 6), it can be seen that the rock layers with high TC are confined between the depths of 2104.5 m and 3458 m, of the Jurassic age, where the TC varies between 2,2 W/m.k and 4,2 W/m.k. This is due to the presence of a large thickness of anhydrite and dolomite and salt in the layers of Malm, Dogger, and Lias ages.

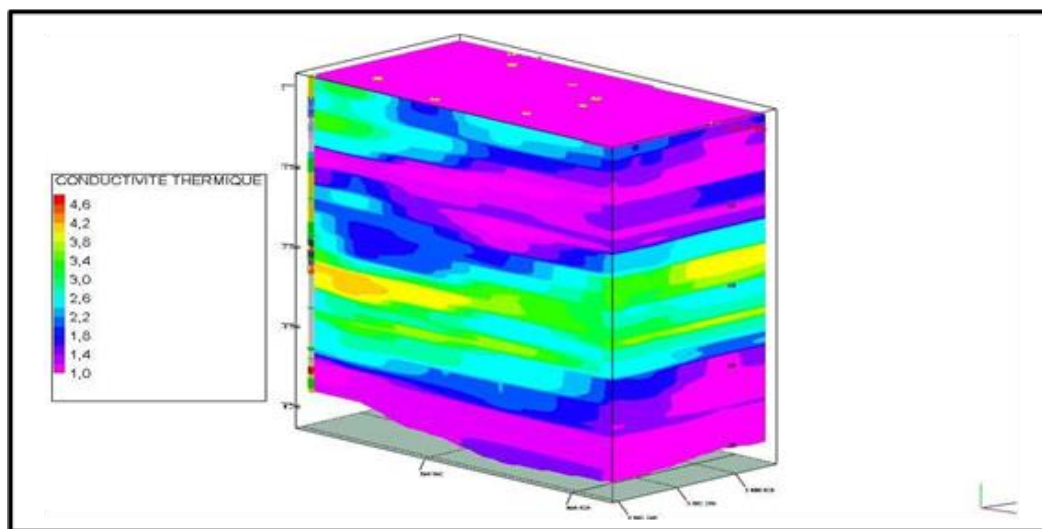


Fig. 6. 3D block of the spatial distribution of thermal conductivity.

As for the low TC zones, they are located in the layers between 3458 m and 4000 m with a TC in the range 1 to 1,8 W/m.k which represents the Triassic (Triassic S4, Lower Clay Triassic, Triassic T2 + T1, Eruptive Triassic, Lower Series Triassic) consisting mainly of clay and sandstone (Table 2). As for the layers located between the surface and a depth of 2104 m, which represents the Cretaceous rocks, they consist mainly of carbonate and evaporite rocks with thermal conductivities varying between 1,4 W/m.k and 2,2 W/m.k.

Table 3: Average thermal conductivity

Level	(k _(s,20)) (W/mK)	Thickness (m)								
		HTBF-1	BRS-3bis	NBOG-1 bis	HTBF-1	BRS-3bis	BBR-2	BEK-1	BBR-2	RAA-1
Salt	6,6	85	00	00	335	223	174	130	84	105
Anhydrite	6	351	349	314	335	746	594	00	00	00
Dolomite	5,5	256	313	122	218	37	80	00	00	00
Gypsum	3	00	35	12	00	00	00	00	00	00
Sandstone	2.7	551	403	384	00	15	26	56	96	28
Limestone	2,5	109	109	291	33	260	185	00	00	00
Marne	2.5	00	41	00	00	00	00	00	00	00
Eruptive rock	1.65	00	00	00	00	00	00	43	74	108
Clay	1.45	335	378	502	257	333	354	217	142	216
Total thickness (m)		1687	1628	1625	1687	1614	1413	456	396	457
(kr)of the		2,845	1,807	1.479						
Cretaceous(W/mK)										
(kr)of the					3.794	3.238	2.802			
Jurassic (W/mK)										
(kr)of the Triassic period (W/mK)								1.983	1.918	1.716

5.4. Thermal Conductivity of Triassic Formations

From the TC map of the Triassic formation in the northern basin of AmguidMessaoud (Fig. 7), one can see that the maximum TC value is found in the extreme southwest of the basin at the HTBF-1 well for the area of Hassi Tayeb Boufas with a value of 2.175 W/m.k while the lowest value was recorded at RAA-1 well is 1,725 W/m.k. In the rest of the basin, the TC ranges from 2,05 W/m.k in the NBOG-1 bis well in the northeast to 1,75 W/m.k in the areas surrounding the ZMT-1 well, (Zemlet El Toufa) in the middle of the basin. From the maximum and minimum TC values of the Triassic formation map, it can be seen that the highest value was recorded at the HTBF-1 well for the area of Hassi Tayeb Boufas with a value of 2.175 W/m.k whereas the lowest value of 1.725 W/m.k was recorded at the RAA-1 well. Through a geological section of each well, we can specify that the first zone of the basin is constituted of 130 m of salt and 10 m of dolomite with a high TC (> 5 W/m.k) and the total thickness of these layers is about 140 m.

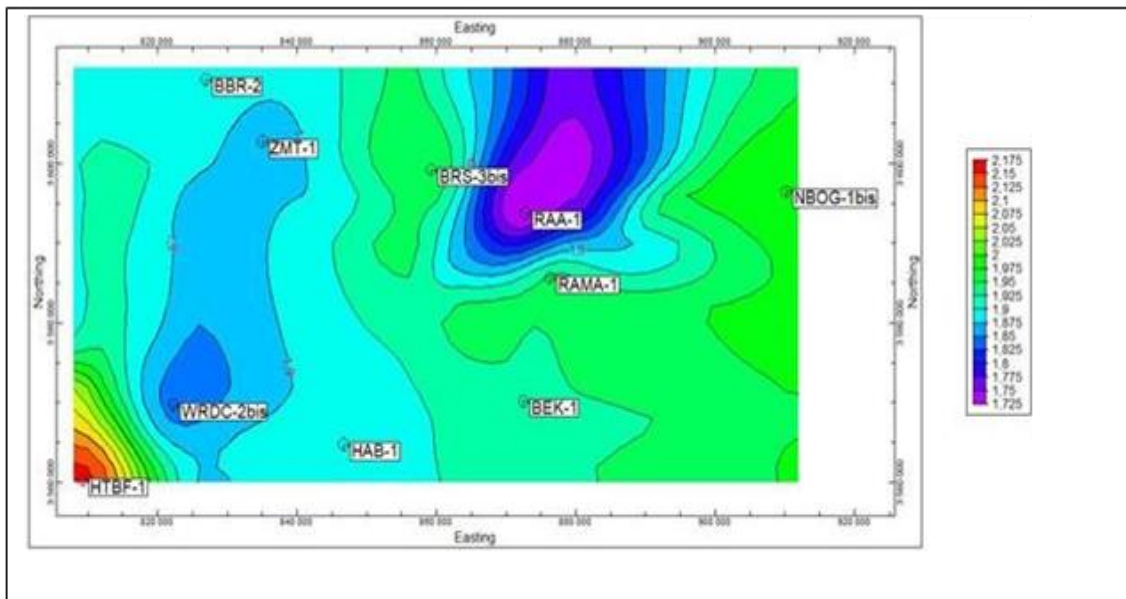


Fig. 7. Thermal conductivity map of the Triassic.

We find that the other layers are made up of 43 m of igneous rock (basalt), 217 m of clay, and 56 m of sandstone, with a total thickness of 316 m. But the TC is less than 3 W/m.k, which is what gives this part a high TC.

On the other hand, in the middle of the basin (well RAA-1), there is a total absence of anhydrite and dolomite, and the thickness of the salt layer decrease to 105 m. Low TC layer such as clay, eruptive rocks, and sandstone have a cumulative thickness of 352 m, or about two-thirds of the total Triassic thickness of 457 m, making it the lowest possible TC zone in the basin. Around the BirBouRouicha BBR-2 well, we note that the Triassic contains only 84 m of salt with the absence of anhydrite and dolomite, and the other layers are less thermally conductive: 74 m of volcanic rocks, 142 m of clay, and 96 m of sandstone with a total of 312m for a conductivity less than 3 W/m.k. It is observed in this part that the low thickness of the rock is offset by the high conductivity and vice versa, therefore the TC can be considered average.

5.5. 2D map of the heat flow at the Triassic reservoir

The basin can be divided into three thermal zones (Fig. 8). The first one is the Hassi Tayeb Boufas area in the southeast, where the HF is between 69 mW/m² and 60 mW/m² (for example HTPF-1 well). The second area is in the middle of the basin and surrounds wells HAB-1 and BBR-2; BRS-3 bis, where the HF value is between 60 mW/m² and 52 mW/m². The third zone of the Far North-East of ZMT-1, (Zemlet El Toufa) up to the area called Rahlet El Aouda and the surrounding wells (RAMA-1, RAA-1), HF values are between 54 mW/m² and 50 mW/m² and the lowest value 50 mW/m² is recorded in Rhourd El Amar-1 at the RAMA-1 well.

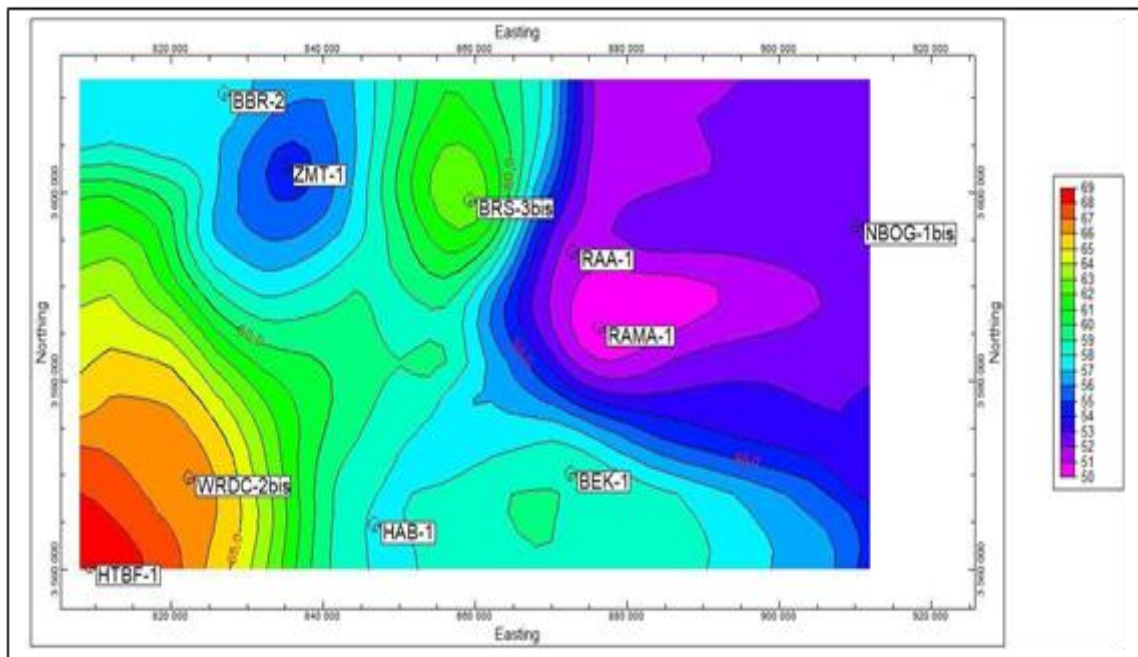


Fig. 8. 2D map of heat flow at the Triassic reservoir.

On the 2D cross-section of the TC model of the region (Fig. 9), it is seen that the lowest possible HF value in the basin 50 mW/m^2 is recorded in Rhourd El Amar-1 at the RAMA-1 well. The Rhourd El Amar-1 formation has a low TC (K_r) ranging from 1.2 mW/m^2 to 3.8 mW/m^2 . These low values can be explained by the lithological composition which contains a thick layer of clay, limestone, sandstone, and eruptive rocks, with a total thickness of 4100 m to give a total thermal resistance of $1672,65 \text{ W/K.m}^2$ for the area of Hassi Tayeb Boufas, in the vicinity of the HTPF-1 well, which has the highest HF value of 69 mW/m^2 , it is characterized by a TC (K_r) between 1.4 W/m.k and 4.6 W/m.k and with a low thickness of layers containing salt, anhydrite, and dolomite, which is characterized by a high TC $k(s,20)$ ($> 5 \text{ W/m.k}$) while the other layers (clay, limestone, sandstone, and eruptive rocks) have a low TC ($< 3 \text{ W/m.k}$). These series of Hassi Tayeb Boufas have a thermal resistance of $745,1387 \text{ W/K.m}^2$, over a total thickness of about 3745 m . This low resistance, compared to the rest of the basin, allows the passage of a large amount of heat from the lower layers to the upper layers and thus the greatest heat flow in the basin. This directly illustrates how thermal conductivity governs the thermal environment. In essence, areas with high thermal conductivity, primarily dominated by thermally conductive rocks such as the basement, exhibit high heat flow, while the opposite holds true as well [28].

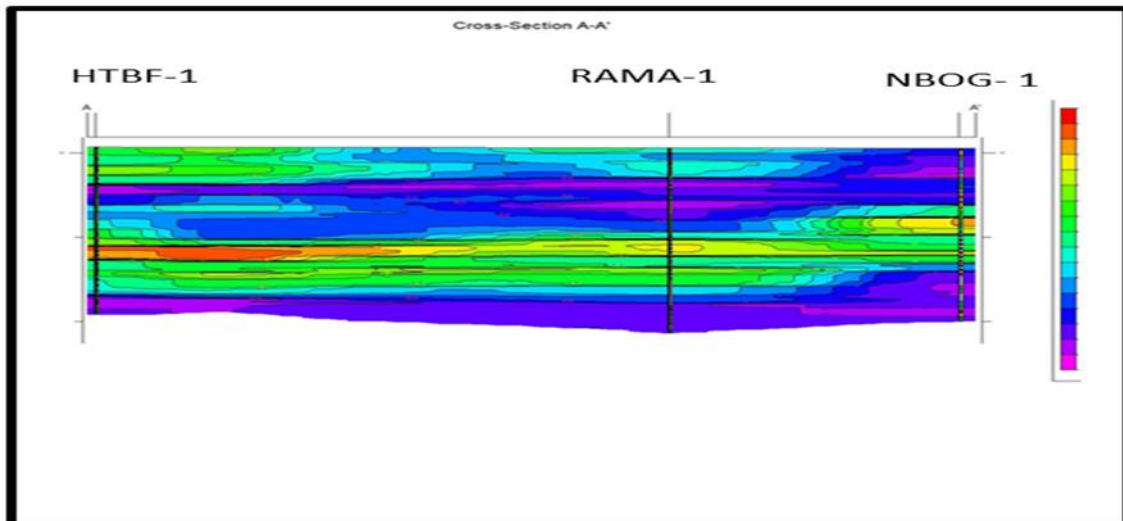


Fig. 9. 2D section of the thermal conductivity model.

6. Conclusion

This research effort is an opportunity to deepen the study of the Algerian Sahara, following the example of many other studies (e.g., SalimaOuali, Hakim Saibi, and others), which aim at measuring the geothermal flows and estimate the potential of geothermal energy resources in the Algerian Sahara.

The AmguidMessaoud basin is a huge oil field covering a total area of 157793km² and belongs to the North African craton.

To create the heat flow map of the AmguidMessaoud Basin, we relied on about 10 wells with complete thermal and geological data files with high-resolution temperature records at depths of about 4000 m.

Calculations of the thermal gradient, surface temperature, thermal conductivity, and heat flux in the entire basin were used as the basis for mapping and 3D modeling of the distribution of the parameters controlling the heat flux in the basin. The results led to the following conclusions:

-The average thermal gradient is 3.275 °C/100m.

-The average heat flux is estimated at 59.5 mW/m² and the highest value of heat flux is 69 mW/m² at the extreme southwest in the HassiTayebBoufas area recorded at the HTPF-1 well.

The lowest value is 50 mW/m² in the northeast in the area of Rhourd El Amar-1 and recorded at the RAMA-1 well.

-We mapped the thermal conductivity for each of the three periods (Triassic, Jurassic, Cretaceous). TC values in the Jurassic range from 2,8 W/m.k to 3,8 W/m.k. This period comprises the most conductive layers involved in heat transfer.

-The Cretaceous period is the least contributing in terms of heat transfer, as it has a TC between 1,4 W/m.k and 2,9 W/m.k.

This study allowed us to better perceive and understand the potential of geothermal energy in the AmguidMessaoud basin in south-eastern Algeria by calculating and determining the temperatures in the oil and gas wells from the data of the oil companies, which allowed us to draw up maps of thermal gradient and heat flow, which show the significant thermal potential in the exploitable depths, which enhances the geothermal energy resources in southern Algeria and in particular in the AmguidMessaoud basin.

Acknowledgments

Thanks are extended to the National Oil Corporation (Sonatrach) for their assistance in collecting and providing oil well data used in this work.

References

- [1] Edwards, M.C. and Chapman, D.S., 2013, geothermal resource assessment of the basin and range province in western Utah. Unpublished report to the Utah Geological Survey, Utah, 121 p. https://geology.utah.gov/docs/geothermal/ngds/pdf/geothermal_B&R.pdf.
- [2] Wyllie, M.R.J., 1963, *The Fundamentals of Well Log Interpretation* (3rd edition). Academic Press, New York, 238. https://books.google.com/books/about/The_Fundamentals_of_Well_Log_Interpretat. Beardsmore, G.R. and Cull, J.P., 2001, *Crustal Heat Flow: a Guide to Measurement and Modelling*. Cambridge University Press, Cambridge, 334 p. <https://doi.org/10.1017/CBO9780511606021>.
- [3] Pasquale, V., Chiozzi, P., Gola, G., and Verdoya, M., 2008, Depth-time correction of petroleum bottom-hole temperatures in the Po Plain, Italy. *Geophysics*, 73, 187–196. <https://doi.org/10.1190/1.2976629>.
- [4] Dowdle, W.L. and Cobb, W.M., 1975, Static formation temperature from well logs – an empirical method. *Journal of Petroleum Technology*, 27, 1326–1330. <https://doi.org/10.2118/5036-PA>.
- [5] Fertl, W.H. and Wichman, P.A., 1977, How to determine static BHT from well log data. *World Oil*, 184, 105–106. [http://refhub.elsevier.com/S0375-6505\(18\)30142-1/sbref0205](http://refhub.elsevier.com/S0375-6505(18)30142-1/sbref0205).
- [6] Luheshi, M.N., 1983, Estimation of formation temperature from borehole measurements. *Geophysical Journal International*, 74, 747–776. <https://academic.oup.com/gji/article/74/3/747/578687>.
- [7] Beck, A.E. and Balling, N., 1988, Determination of virgin rock temperatures. In: Haenel, R., Rybach, L., Stegena, L. (eds) *Handbook of Terrestrial Heat-Flow Density Determination*. Solid Earth Sciences Library, vol 4. Springer, Dordrecht. https://doi.org/10.1007/978-94-009-2847-3_3.

- [8] Ali, S., Musto-Onuoha, K. and Orazulike, D., 2005, Bottom-hole temperature correction – the Chad Basin, N.E., Nigeria case study. *Global Journal of Geological Sciences*, 3, 133–142. <https://doi.org/10.4314/GJGS.V3I2.18720>.
- [9] Takherist, D., 1990, Structure crustale, subsidence mésozoïque et flux de chaleur dans les bassins nord-sahariens (Algérie) : apport de la gravimétrie et des données de puits. Ph.D. Thesis, University of Montpellier, Montpellier, 236 p. <http://www.theses.fr/1990MON20052>.
- [10] Aït-Salem, H., 1992, Le Trias détritique de l'Oued Mya (Sahara algérien). Sédimentation estuarienne, diagenèse et porogenèse, potentialités pétrolières. *Travaux et Documents Des Laboratoires de Géologie de Lyon*, 120, 171 p. <https://doi.org/10.1111/J.1365-246X.2007.03403.X/2/170-2-913-TBL002.JPEG>.
- [11] Ouali, S., Khellaf, A., and Baddari, K., 2007, Etude des ressources géothermiques du sud algérien. *Revue Des Energies Renouvelables*, 10, 407–414. https://www.cder.dz/download/Art10-3_10.pdf.
- [12] Pommier, G. and Balducci, A.M., 1968, Cambrian oil field of Hassi Messaoud, Algeria. *AAPG Bulletin*, 52, 545–545. <https://doi.org/10.1306/5D25C39F-16C1-11D7-8645000102C1865D>.
- [13] Lachenbruch, A. and Brewer, M., 1959, Dissipation of the temperature effect of drilling a well in Arctic Alaska. *Bulletin of the United States Geological Survey*, 1083-C, 73–109. [http://refhub.elsevier.com/S0012-8252\(16\)30462-7/rf0340](http://refhub.elsevier.com/S0012-8252(16)30462-7/rf0340)
- [14] Zarhloule, Y., 2004, Le gradient géothermique profond du Maroc: détermination et cartographie. *Bulletin de l'Institut Scientifique, Section Sciences de la Terre*, 26, 11–25. [http://www.israbat.ac.ma/wp-content/uploads/2015/03/02-%20Zarhloule%20\(11-25\).pdf](http://www.israbat.ac.ma/wp-content/uploads/2015/03/02-%20Zarhloule%20(11-25).pdf)
- [15] Goutorbe, B., Lucazeau, F., and Bonneville, A., 2007, Comparison of several BHT correction methods: A case study on an Australian data set. *Geophysical Journal International*, 170, 913–922. https://www.persee.fr/doc/geoly_0750-6635_1992_mon_120_1_1768
- [16] Ouali, S., 2009, Thermal conductivity in relation to porosity and geological stratigraphy. Report 23, Geothermal training programme, United Nations University, Reykjavík, 18p. <https://api.semanticscholar.org/CorpusID:19890327>
- [17] Kouider, M.H. and Nezli, I.E., 2019, The geothermal potentialities of Southern Algeria. *AIP Conference Proceedings*, 2123, 1–11. <https://doi.org/10.1063/1.5117036/700892>.
- [18] Henrikson, A. and Chapman, D.S., 2002, Terrestrial heat flow in Utah. Report of Department of Geology and Geophysics, University of Utah, Salt Lake City, Utah, 47p. https://ugspub.nr.utah.gov/publications/open_file_reports/ofr-431/ofr-431_terrestrial-heat-flow-utah.pdf Saibi, H., 2009,

- Geothermal resources in Algeria. *Renewable and Sustainable Energy Reviews*, 13, 2544–2552. <https://doi.org/10.1016/J.RSER.2009.06.019>.
- [19] Chapman, D.S., Keho, T.H., Bauer, M.S., and Picard, M.D., 2012, Heat flow in the Uinta Basin determined from bottom hole temperature (BHT) data. *Geophysics*, 49, 453–466. doi: <https://doi.org/10.1190/1.1441680>.
- [20] Tyoh, A.A., Uko, E.D., Ayanninuola, O.S., and Davies, O.A., 2021, Effects of near-Surface air temperature on sub-surface geothermal gradient and heat flow in Bornu-Chad basin, Nigeria. *International Journal of Terrestrial Heat Flow and Applied Geothermics*, 4, 95–102. <https://doi.org/10.31214/IJTHFA.V4I1.68>.
- [21] Kappelmeyer, O. and Haenel, R., 1974, *Geothermics With Special Reference to Application*. Gebrüder Borntraeger, Berlin, 238p. http://www.schweizerbart.de/publications/detail/isbn/9783443130060/Kappelmeyer_Haenel_Geothermics_Geoex
- [22] Frederic, B., David S.C., and Sylvie, D., 1990, Estimating thermal conductivity in sedimentary basins using lithologic data and geophysical well logs (1). *AAPG Bulletin*, 74, 1459–1477. DOI: <https://doi.org/10.1306/0C9B2501-1710-11D7-8645000102C1865D>
- [23] Kwaya, M.Y., Kurowska, E., Arabi, A.S., Kwaya, M.Y., Kurowska, E., and Arabi, A.S., 2016, Geothermal gradient and heat flow in the Nigeria sector of the Chad basin, Nigeria. *Computational Water, Energy, and Environmental Engineering*, 5, 70–78. <https://doi.org/10.4236/CWEEE.2016.52007>.
- [24] Li, Z.X., Xu, M., Zhao, P., Sun, Z.X., and Zhu, C.Q., 2013, Geothermal regime and hydrocarbon kitchen evolution in the Jiangnan Basin. *Science China Earth Sciences*, 56, 240–257. <https://doi.org/10.1007/s11430-012-4462-8>.
- [25] Emujakporue, G.O. and Ekine, A.S., 2014, Determination of geothermal gradient in the eastern Niger delta sedimentary basin from bottom hole temperatures. *Journal of Earth Sciences and Geotechnical Engineering*, 4, 1792–9660. <https://www.scienpress.com/download.asp?ID=1238>.
- [26] Putra, S.D.H., Suryantini, J., and Srigutomo, W., 2016, Thermal modeling and heat flow density interpretation of the onshore Northwest Java Basin, Indonesia. *Geotherm Energy* 4, 1–24. <https://doi.org/10.1186/s40517-016-0052-x>.